Inorganic Chemistry

Article

A Quantum Chemistry View on Two Archetypical Paramagnetic Pentacoordinate Nickel(II) Complexes Offers a Fresh Look on Their NMR Spectra

Enrico Ravera,* Lucia Gigli, Barbara Czarniecki, Lucas Lang, Rainer Kümmerle, Giacomo Parigi, Mario Piccioli, Frank Neese, and Claudio Luchinat*

Read Online

ACCESS | Metrics & More | Article Recommendations | Supporting Information

ABSTRACT: Quantum chemical methods for calculating paramagnetic NMR observables are becoming increasingly accessible and are being included in the inorganic chemistry practice. Here, we test the performance of these methods in the prediction of proton hyperfine shifts of two archetypical high-spin pentacoordinate nickel(II) complexes (NiSAL-MeDPT and NiSAL-HDPT), which, for a variety of reasons, turned out to be perfectly suited to challenge the predictions to the finest level of detail. For NiSAL-MeDPT, new NMR experiments yield an assignment that perfectly matches the calculations. The slightly different hyperfine shifts from the two "halves" of the molecules related by a pseudo-C_2 axis, which are experimentally divided into two well-defined spin systems, are also straightforwardly distinguished by the calculations. In the case of NiSAL-HDPT, for which no X-ray structure is available, the quality of the calculations allowed us to refine its structure using as a starting template the structure of NiSAL-MeDPT.
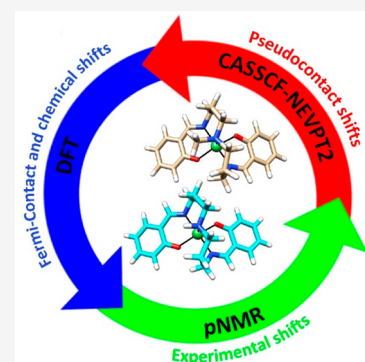
INTRODUCTION

Quantum chemical analysis of paramagnetic shifts (pNMR) in terms of the electronic structure of metal centers is gathering momentum, thanks to the effort of computational and experimental groups: the understanding of the electronic structure allows for a deeper understanding of the magnetic behavior of paramagnetic systems for the spectroscopic characterization of inorganic compounds,[1−9] for structure analysis in bioinorganic chemistry,[10−14] and also in view of the development of (e.g.) single-ion magnets or qubits.[15−23] With this work, we want to challenge state-of-the-art QC methods to accurately predict hyperfine shifts (both contact and pseudo-contact) for an inorganic system the NMR properties of which have been studied over decades. We select complexes of nickel(II) coordinated by pentadentate salicylaldiminates with dipropylenetriamine bridges (SAL-DPT), such as NiSAL-MeDPT and NiSAL-HDPT (SAL = salicylaldiminate; DPT = dipropylenetriamine), which are archetypical of high-spin pentacoordinate complexes of this metal (Figure 1), being the first to be designed to enforce this—at the time—unusual coordination and spin state in nickel(II).[24] These complexes have very particular spectroscopic features:

(1) The ^{1}H NMR spectra may span almost 1000 ppm (Figure 1)[25,26] and, therefore, are used as benchmarks for NMR hardware development and testing.[27]

(2) The hyperfine shifts originate from both contact and pseudocontact contributions, none of the two being negligible for some protons.

(3) Being intrinsically not symmetric, there are no magnetically equivalent protons.

(4) However, the two enantiomers can interconvert into one another; therefore, the signal of each proton (except for those on the apical nitrogen) is always linked by chemical exchange to the signal of the proton that is in the mirror position.

In addition, the HDPT derivative does not easily crystallize; therefore, there is no structure available for it.

All these features make these complexes an optimal benchmark for testing the prediction of QC methods: pNMR QC methods are not always in agreement with one another, as far as the calculation of the pseudocontact shift (PCS) contribution is concerned.[28,29] A recent QC treatment differs from the semiempirical approach based on the Spin Hamiltonian parameters for the inclusion of the nucleus-orbit coupling (called in the literature Paramagnetic Spin-Orbit contribution), and this difference breaks the link between the pseudocontact shifts and the magnetic susceptibility anisotropy tensor.[29] This QC-based approach has been increasingly used to describe inorganic and bio-inorganic systems,[30−33,14] although the
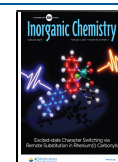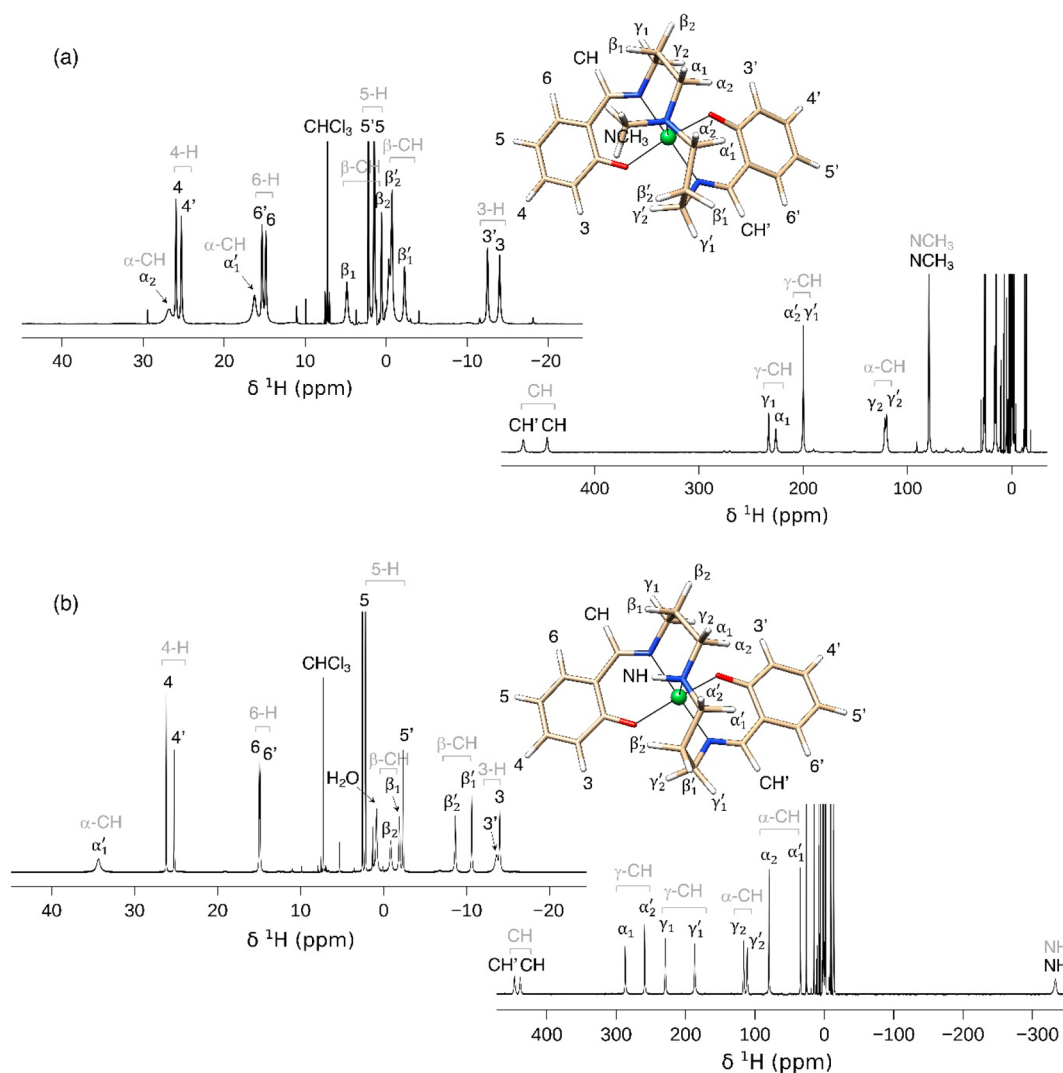
Figure 1. Structure and ^1H NMR spectra acquired at 1200 MHz of NiSAL-MeDPT (panel a) and NiSAL-HDPT (panel b). The assignment indicated in gray is the one proposed by Sacconi and LaMar; the assignment in black is the one obtained in the present work.

discrepancy was not completely understood. The inclusion of further terms in the rigorous QC treatment has allowed for the resolution of the ambiguity,[34] demonstrating that the pseudocontact shift is indeed dependent on the magnetic susceptibility tensor and thus providing a definitive proof of the McConnell–Robertson (or Kurland–McGarvey) equation[35,36]

$$\delta_{PCS}\ (ppm) = \frac{1}{12\pi r^5} 10^6 Tr[3\mathbf{r}\mathbf{r}^{\mathbf{T}} \cdot \chi - r^2 \chi] \tag{1}$$

where χ is the magnetic susceptibility anisotropy tensor, and $\mathbf{r}$ is the metal–nucleus distance vector.

For the above reasons, we have performed a quantum chemical analysis of the ^1H NMR spectra of NiSAL-MeDPT and NiSAL-HDPT and verified the computational predictions by new experiments.

■ METHODS

Structure. The 3D structure of NiSAL-MeDPT was obtained from the CCDC (accession number 1254189, ID: SAIMNI10).[37] The structure was subjected to refinement at the DFT level of theory, with the B3LYP functional[38−41] using Ahlrichs polarized basis set def2-TZVP[42,43] and Grimme's dispersion correction D3.[44,45] The resolution of identity

approximation[46,47] was employed with auxiliary basis set def2-TZVP/J in order to speed up the calculations. CPCM implicit solvent (chloroform) was used.[48] The structure of NiSAL-HDPT is not available and, therefore, it has been obtained by substituting the methyl group with a hydrogen atom and repeating the geometry optimization. All calculations were carried out using the ORCA 4.2.1 quantum chemistry package.[49,50]

Shifts. The "diamagnetic" contribution, i.e., the chemical shift net of the contributions of the coupling with the unpaired electron spins, has been calculated at the same level of theory as the geometry optimization, using gauge-invariant atomic orbitals and referencing to tetramethylsilane calculated under the same conditions.

For the calculation of the PCS, we have used the McConnell–Robertson (or Kurland–McGarvey) equation (eq 1),[35,36] using the magnetic susceptibility tensor computed with the state-averaged complete active space self-consistent field (SA-CASSCF),[51,52] accounting for the dynamic correlation by N-electron valence perturbation theory to the second order (NEVPT2)[53,54] as described in detail in ref 55. The segmented all-electron relativistically contracted version of Ahlrichs polarized basis sets def2-TZVP[56,57] and the second-order
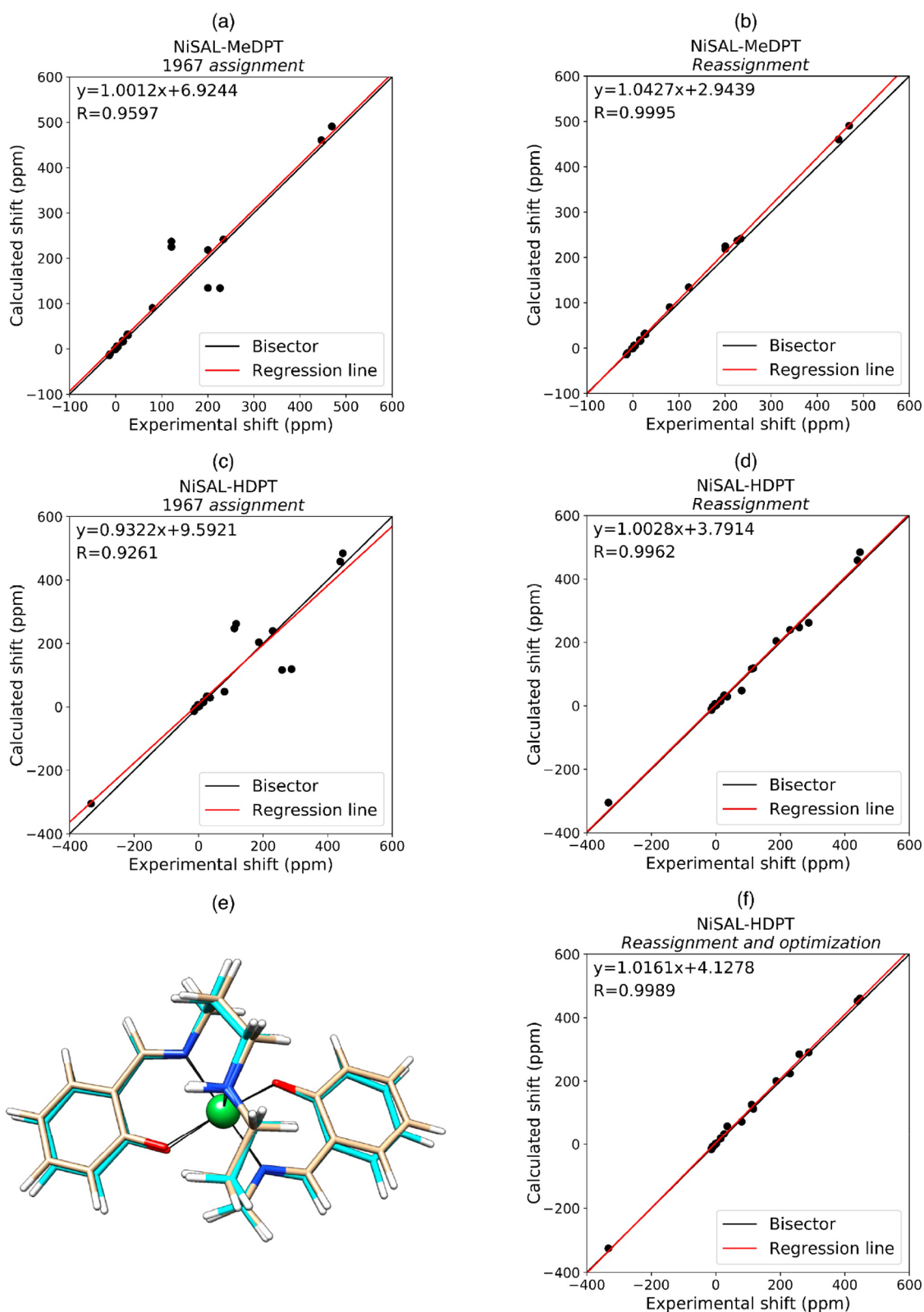
Figure 2. Agreement between experimental and QC calculated shifts for NiSAL-MeDPT and NiSAL-HDPT, with the assignment proposed by Sacconi and LaMar (panels a and c),[25] and the theory-based reassignment (panels b and d), respectively. Agreement between experimental and QC calculated shifts of the NiSAL-HDPT optimized structure (panel f) and comparison between initial (beige) and optimized (cyan) NiSAL-HDPT structure (panel e). The QC calculated shifts, together with their FC, PCS, and diamagnetic contributions, and the experimental shifts of NiSAL-MeDPT and optimized NiSAL-HDPT are reported in Tables S1 and S2, respectively. The linear regression lines are shown in red, and the equation and correlation coefficient are given in the figures. Bisecting lines are shown in black as a guide to the eye.

Douglas−Kroll−Hess Hamiltonian (DKH)[58] were employed to account for the scalar relativistic effects. The active space was chosen to contain eight electrons in the five nickel 3d-based molecular orbitals. All microstates arising from the d^8 configuration were included in the calculation. The spin-orbit coupling was treated using the spin-orbit mean field approximation as implemented in ORCA.[59] Note that the Fermi contact tensor cannot be obtained properly by that same approach since the CASSCF wave function lacks spin-polarization and the NEVPT2 correction only pertains to the energy. Hence, the Fermi-Contact (FC) contribution to the para-magnetic shift was calculated at the same level of DFT as used for the geometry and the diamagnetic chemical shift calculation, but accounting for scalar relativistic effects through the DKH Hamiltonian.[58] Property calculations involving the application of non-relativistic operators on relativistic wavefuctions include picture change effects,[60] and a finite nucleus model.[61] A note on the calculation of the contact shift term: ORCA provides the hyperfine coupling constant A in MHz; the FC shift (in ppm) is therefore given by δ_{FC} (ppm) $= 2\pi 10^{12} A g_{iso} \mu_B S(S + 1)/(3\gamma_H k_B T)$.[62] The value of the isotropic g-shift is taken from the DFT calculation for consistency: DFT has a tendency to overestimate electron delocalization,[63,64] whereas it under-estimates the molecular g-matrix because of the lack of configuration interaction and dynamical correlation.[63,65,66] The isotropic g-shift calculated at the multireference level is about 6−10% larger than that calculated at the DFT level in the considered systems. Consequently, the contact shift values would be increased by the same amount.

■ EXPERIMENTS

The complexes were prepared as described in ref 24, recrystallized from dichloromethane/toluene and finally dissolved in deuterated chloro-form for performing the NMR experiments. *Caution!The health and environment effects of the reported complexes have not been characterized. Nickel(II) complexes may cause sensitization by skin contact; there is limited evidence of carcinogenic effects and may cause long-term adverse effects in the aquatic environment. Chloroform is a suspect carcinogenic agent.*

The NMR spectra were recorded on three instruments:

(1) A Bruker Avance III spectrometer operating at 400 MHz ^{1}H Larmor frequency (9.4 T) using a 5 mm, ^{1}H selective probe dedicated to paramagnetic systems (the nutation frequency of the hard pulse is ca. 90 kHz).

(2) A Bruker Avance NEO spectrometer operating at 1.2 GHz with a 28.2 T HTS/LTS hybrid magnet, using a 3 mm, triple resonance TCI cryo-probehead (the nutation frequency of the hard pulse is ca. 37 kHz; therefore, the excitation was achieved with a small flip-angle 200 ns pulse length).

(3) A Bruker Benchtop NMR Fourier 80 device (1.9 T, the nutation frequency of the hard pulse is ca. 27 kHz; therefore, uniform excitation can be achieved over the considered chemical shift range).

■ RESULTS AND DISCUSSION

In line with the expectations, the metal coordination in the DFT-refined structures of both NiSAL-MeDPT (Figure S1, panels a, d, g) and NiSAL-HDPT (Figure S1, panels b, e, h) is square pyramidal, with a slight trigonal distortion: the two oxygen donors are bent out of plane by about 12°. The effective magnetic moment obtained with CASSCF-NEVPT2 is in line with the experimental one: 3.33 B.M. for NiSAL-MeDPT (experimental 3.34 B.M.) and 3.32 B.M. for NiSAL-MeDPT (experimental 3.32 B.M.).

The first observation is that most of the calculated shifts agree rather well with the experimental data of both complexes using the assignments reported in ref 25 (Figure 2, panels a and c). However, if the assignment of the methylene signals is reversed, the agreement becomes nearly perfect for NiSAL-MeDPT (Figure 2, panel b) and reasonably good also for NiSAL-HDPT (Figure 2, panel d).

We have used NiSAL-HDPT to confirm this theory-based reassignment because of the larger separation of the resonances: a COSY spectrum recorded at 80 MHz shows three crosspeaks (Figure S2):

(a) 288 ppm to 79.9 ppm.

(b) 259 ppm to 35.2 ppm.

(c) 79.9 ppm to −0.82 ppm.

Crosspeaks a and b are unambiguously attributable to two geminal pairs, whereas c links one of the alpha methylene protons to the vicinal beta methylene protons, establishing an unambiguous connectivity. Finally, the presence of a strong NOE response of the resonance at 288 ppm to the irradiation of the one at 229 ppm and the presence of an exchange response of the resonance at −1.9 ppm to the irradiation of the one at −8.5 (Figure S3) remove all the ambiguities in the two propylene branches, but that between the two signals at 117 and 111 ppm, which could not be resolved experimentally. The connectivity obtained in this way is perfectly compatible with the assignment obtained from the comparison between computed and experimental spectra.

The COSY spectrum acquired at 400 MHz allows for tracing the connectivity in the two rings (Figure S4), resulting in a pattern of the type (from downfield to upfield, Figure 1) 4-4′; 6′-6; 5-5′; 3-3′, which is again confirmed by the calculations.

In a situation in which the assignment obtained from the calculations is fully confirmed by the experimental data, the reliability of the theoretical calculations is strongly supported. On this basis it is possible to interpret the small discrepancies between observed and calculated shifts obtained for the HDPT derivative (whose structure is not experimentally determined but only modeled on that of the MeDPT derivative) in terms of minor structural changes. Most of the deviation relates to the alpha methylene protons, where the calculation appears to be underestimating the contact contribution, especially for α_1 and α_2, whereas α'_1 and α'_2 deviate much less. Bearing in mind that this structure is not experimental, it is reasonable to think that the structure may need to be altered. Therefore, we have performed a very coarse scan (9 steps, ca. 7° for each) of the dihedral angles formed by α_1 with its carbon, the apical nitrogen, and the nickel ion, around the initial position of −172.9° (187.1°) found in the optimized structure. From a qualitative viewpoint, this angle is likely the strongest determinant of the contact shift because it controls the overlap of the hydrogen nuclei with the orbitals of the donor atom overlapped with the metal orbitals bearing the unpaired electron.[67−70,62,71] When α_1 is 172.9° (Figure 2, panel e, and Figure S1, panels c, f, i), the agreement to the experimental data becomes very good and comparable in quality to that of the MeDPT derivative (Figure 2, panel f).

We feel that a further comment is needed on the strategy we adopted in this work. In line with recent literature on the calculation of magnetic,[72,73] EPR, and NMR proper-ties,[14,17,18,21,74,75,30] we apply single point calculations per-formed on minimum positions achieved by optimization at the DFT level; therefore, the results do not include effects that are

due to mobility or dynamics. The latter are, indeed, very important in the calculation of relaxation properties.[76−78] Conversely, to calculate shift/susceptibility values, a symmetric averaging around a single minimum position is not expected to yield average values significantly different from the values calculated in the average position. Calculations of magnetic properties from structural ensembles are currently too demanding for routine applications. However, we expect that, with the improvement in the computers and in the computational tools, all the calculations needed to average among the accessible states (e.g., calculated through *ab initio* molecular dynamics) will become feasible in the near future, providing access not only to thermal effects but also to solvent effects, as recently discussed in refs 79 and 80.

CONCLUSIONS

The first evidence of the existence of five coordination in transition metal complexes and, in particular, of high-spin 5-coordinate nickel(II) complexes[81−83] was put forward in the 1960s by the Institute of General Chemistry of the University of Florence, founded and directed by Luigi Sacconi. To gain further insight into this unusual coordination, Sacconi, together with Ivano Bertini in 1966, developed the SAL-DPT class of ligands.[24] These pentadentate ligands are sufficiently rigid and bulky to enforce pentacoordination and to sterically discourage the access to the sixth coordination position, and the N- and O-donors favor the high-spin configuration.[84] They were among the first paramagnetic compounds ever addressed by NMR,[25] and therefore extremely well characterized. However, the present calculations gave a strong hint toward reassigning the signals, which could be verified by measuring at low field, and provided a complete site-specific assignment that would have not been achievable on a purely experimental basis. This work thus demonstrates that the combined use of experiments and calculations can reveal details that are not easily accessible by experiment alone and suggests how to perform the experiments to resolve ambiguities. Finally, the minor, but significant, refinement of the HDPT derivative structural model suggests that the quality of QC calculations has reached such a maturity so as to experimentally determine the structure of metal complexes starting from homologous compounds.

ASSOCIATED CONTENT

ⓈI Supporting Information

The Supporting Information is available free of charge at https://pubs.acs.org/doi/10.1021/acs.inorgchem.0c03635.

Different views of the structures, and COSY and 1D NOE spectra (PDF)

AUTHOR INFORMATION

Corresponding Authors

Enrico Ravera − *Department of Chemistry "Ugo Schiff", University of Florence, 50019 Sesto Fiorentino, Italy; Magnetic Resonance Center, University of Florence and Consorzio Interuniversitario Risonanze Magnetiche di Metalloproteine, 50019 Sesto Fiorentino, Italy;* ⓞ orcid.org/0000-0001-7708-9208; Email: ravera@cerm.unifi.it

Claudio Luchinat − *Department of Chemistry "Ugo Schiff", University of Florence, 50019 Sesto Fiorentino, Italy; Magnetic Resonance Center, University of Florence and Consorzio Interuniversitario Risonanze Magnetiche di Metalloproteine,*

50019 Sesto Fiorentino, Italy; ⓞ orcid.org/0000-0003-2271-8921; Email: luchinat@cerm.unifi.it

Authors

Lucia Gigli − *Department of Chemistry "Ugo Schiff", University of Florence, 50019 Sesto Fiorentino, Italy; Magnetic Resonance Center, University of Florence and Consorzio Interuniversitario Risonanze Magnetiche di Metalloproteine, 50019 Sesto Fiorentino, Italy*

Barbara Czarniecki − *Bruker Biospin Corporation, 8117 Fällanden, Switzerland*

Lucas Lang − *Max-Planck-Institut für Kohlenforschung, 45470 Mülheim an der Ruhr, Germany;* ⓞ orcid.org/0000-0002-5796-1641

Rainer Kümmerle − *Bruker Biospin Corporation, 8117 Fällanden, Switzerland*

Giacomo Parigi − *Department of Chemistry "Ugo Schiff", University of Florence, 50019 Sesto Fiorentino, Italy; Magnetic Resonance Center, University of Florence and Consorzio Interuniversitario Risonanze Magnetiche di Metalloproteine, 50019 Sesto Fiorentino, Italy;* ⓞ orcid.org/0000-0002-1989-4644

Mario Piccioli − *Department of Chemistry "Ugo Schiff", University of Florence, 50019 Sesto Fiorentino, Italy; Magnetic Resonance Center, University of Florence and Consorzio Interuniversitario Risonanze Magnetiche di Metalloproteine, 50019 Sesto Fiorentino, Italy;* ⓞ orcid.org/0000-0001-9882-9754

Frank Neese − *Max-Planck-Institut für Kohlenforschung, 45470 Mülheim an der Ruhr, Germany;* ⓞ orcid.org/0000-0003-4691-0547

Complete contact information is available at:
https://pubs.acs.org/10.1021/acs.inorgchem.0c03635

Author Contributions

The manuscript was written through contributions of all authors. All authors have given approval to the final version of the manuscript.

Notes

The authors declare no competing financial interest.

ACKNOWLEDGMENTS

REFERENCES

(1) Szalontai, G.; Csonka, R.; Speier, G.; Kaizer, J.; Sabolović, J. Solid-State NMR Study of Paramagnetic Bis(Alaninato-κ_2N,O)Copper(II) and Bis(1-Amino(Cyclo)Alkane-1-Carboxylato-κ_2N,O)Copper(II) Complexes: Reflection of Stereoisomerism and Molecular Mobility in ^{13}C and ^{2}H Fast Magic Angle Spinning Spectra. *Inorg. Chem.* **2015**, 54 (10), 4663−4677.

(2) Levin, K.; Kroeker, S. Probing Jahn–Teller Distortions in $Mn(Acac)_3$ through Paramagnetic Interactions in Solid-State MAS NMR. *Solid State Nucl. Magn. Reson.* **2019**, *101*, 101−109.

(3) Rouf, S. A.; Jakobsen, V. B.; Mareš, J.; Jensen, N. D.; McKenzie, C. J.; Vaara, J.; Nielsen, U. G. Assignment of Solid-State ^{13}C and ^1H NMR Spectra of Paramagnetic Ni(II) Acetylacetonate Complexes Aided by First-Principles Computations. *Solid State Nucl. Magn. Reson.* **2017**, *87*, 29−37.

(4) Andersen, A. B. A.; Pyykkönen, A.; Jensen, H. J. A.; McKee, V.; Vaara, J.; Nielsen, U. G. Remarkable Reversal of ^{13}C-NMR Assignment in d^1, d^2 Compared to d^8, d^9 Acetylacetonate Complexes: Analysis and Explanation Based on Solid-State MAS NMR and Computations. *Phys. Chem. Chem. Phys.* **2020**, *22* (15), 8048−8059.

(5) Michaelis, V. K.; Greer, B. J.; Aharen, T.; Greedan, J. E.; Kroeker, S. Determining Electron Spin-Transfer Mechanisms in Paramagnetic Ba_2YMO_6 (M = Mo, Re, Ru) Double Perovskites by ^{89}Y and ^{137}Ba MAS NMR Spectroscopy. *J. Phys. Chem. C* **2012**, *116* (44), 23646−23652.

(6) Gendron, F.; Sharkas, K.; Autschbach, J. Calculating NMR Chemical Shifts for Paramagnetic Metal Complexes from First-Principles. *J. Phys. Chem. Lett.* **2015**, *6* (12), 2183−2188.

(7) Martin, B.; Autschbach, J. Temperature Dependence of Contact and Dipolar NMR Chemical Shifts in Paramagnetic Molecules. *J. Chem. Phys.* **2015**, *142* (5), 054108.

(8) Autschbach, J.; Patchkovskii, S.; Pritchard, B. Calculation of Hyperfine Tensors and Paramagnetic NMR Shifts Using the Relativistic Zeroth-Order Regular Approximation and Density Functional Theory. *J. Chem. Theory Comput.* **2011**, *7* (7), 2175−2188.

(9) Ooms, K.; Polenova, T.; Shough, A.-M.; Doren, D. J.; Nash, M. J.; Lobo, R. F. Identification of Mixed Valence Vanadium in ETS-10 Using Electron Paramagnetic Resonance, 51V Solid-State Nuclear Magnetic Resonance, and Density Functional Theory Studies. *J. Phys. Chem. C* **2009**, *113* (24), 10477−10484.

(10) Shokhirev, N. V.; Walker, F. A. Analysis of the Temperature Dependence of the ^1H Contact Shifts in Low-Spin Fe(III) Model Hemes and Heme Proteins: Explanation of "Curie" and "Anti-Curie" Behavior within the Same Molecule. *J. Phys. Chem.* **1995**, *99* (50), 17795−17804.

(11) Bertini, I.; Luchinat, C.; Parigi, G. The Hyperfine Shifts in Low Spin Iron(III) Hemes: A Ligand Field Analysis. *Eur. J. Inorg. Chem.* **2000**, *2000*, 2473−2480.

(12) Lin, I. J.; Xia, B.; King, D. S.; Machonkin, T. E.; Westler, W. M.; Markley, J. L. Hyperfine-Shifted ^{13}C and ^{15}N NMR Signals from Clostridium Pasteurianum Rubredoxin: Extensive Assignments and Quantum Chemical Verification. *J. Am. Chem. Soc.* **2009**, *131* (42), 15555−15563.

(13) Liptak, M. D.; Wen, X.; Bren, K. L. NMR and DFT Investigation of Heme Ruffling: Functional Implications for Cytochrome c. *J. Am. Chem. Soc.* **2010**, *132* (28), 9753−9763.

(14) Bertarello, A.; Benda, L.; Sanders, K.; Pell, A. J.; Knight, M. J.; Pelmenschikov, V.; Gonnelli, L.; Felli, I. C.; Kaupp, M.; Emsley, L.; Pierattelli, R.; Pintacuda, G. Picometer Resolution Structure of the Coordination Sphere in the Metal-Binding Site in a Metalloprotein by NMR. *J. Am. Chem. Soc.* **2020**, *142*, 16757−16765.

(15) Novikov, V. V.; Pavlov, A. A.; Belov, A. S.; Vologzhanina, A. V.; Savitsky, A.; Voloshin, Y. Z. Transition Ion Strikes Back: Large Magnetic Susceptibility Anisotropy in Cobalt(II) Clathrochelates. *J. Phys. Chem. Lett.* **2014**, *5* (21), 3799−3803.

(16) Novikov, V. V.; Pavlov, A. A.; Nelyubina, Y. V.; Boulon, M.-E.; Varzatskii, O. A.; Voloshin, Y. Z.; Winpenny, R. E. P. A Trigonal Prismatic Mononuclear Cobalt(II) Complex Showing Single-Molecule Magnet Behavior. *J. Am. Chem. Soc.* **2015**, *137* (31), 9792−9795.

(17) Vonci, M.; Mason, K.; Suturina, E. A.; Frawley, A. T.; Worswick, S. G.; Kuprov, I.; Parker, D.; McInnes, E. J. L.; Chilton, N. F. Rationalization of Anomalous Pseudocontact Shifts and Their Solvent Dependence in a Series of C_3-Symmetric Lanthanide Complexes. *J. Am. Chem. Soc.* **2017**, *139* (40), 14166−14172.

(18) Hiller, M.; Krieg, S.; Ishikawa, N.; Enders, M. Ligand-Field Energy Splitting in Lanthanide-Based Single-Molecule Magnets by NMR Spectroscopy. *Inorg. Chem.* **2017**, *56* (24), 15285−15294.

(19) Morita, T.; Damjanović, M.; Katoh, K.; Kitagawa, Y.; Yasuda, N.; Lan, Y.; Wernsdorfer, W.; Breedlove, B. K.; Enders, M.; Yamashita, M. Comparison of the Magnetic Anisotropy and Spin Relaxation Phenomenon of Dinuclear Terbium(III) Phthalocyaninato Single-Molecule Magnets Using the Geometric Spin Arrangement. *J. Am. Chem. Soc.* **2018**, *140* (8), 2995−3007.

(20) Pavlov, A. A.; Nehrkorn, J.; Pankratova, Y. A.; Ozerov, M.; Mikhalyova, E. A.; Polezhaev, A. V.; Nelyubina, Y. V.; Novikov, V. V. Detailed Electronic Structure of a High-Spin Cobalt(II) Complex Determined from NMR and THz-EPR Spectroscopy. *Phys. Chem. Chem. Phys.* **2019**, *21* (16), 8201−8204.

(21) Suturina, E. A.; Mason, K.; Botta, M.; Carniato, F.; Kuprov, I.; Chilton, N. F.; McInnes, E. J. L.; Vonci, M.; Parker, D. Periodic Trends and Hidden Dynamics of Magnetic Properties in Three Series of Triazacyclononane Lanthanide Complexes. *Dalton Trans.* **2019**, *48* (23), 8400−8409.

(22) Hiller, M.; Sittel, T.; Wadepohl, H.; Enders, M. A New Class of Lanthanide Complexes with Three Ligand Centered Radicals: NMR Evaluation of Ligand Field Energy Splitting and Magnetic Coupling. *Chem. - Eur. J.* **2019**, *25* (45), 10668−10677.

(23) Parker, D.; Suturina, E. A.; Kuprov, I.; Chilton, N. F. How the Ligand Field in Lanthanide Coordination Complexes Determines Magnetic Susceptibility Anisotropy, Paramagnetic NMR Shift, and Relaxation Behavior. *Acc. Chem. Res.* **2020**, *53* (8), 1520−1534.

(24) Sacconi, L.; Bertini, I. High-Spin Five-Coordinated 3d Metal Complexes with Pentadentate Schiff Bases. *J. Am. Chem. Soc.* **1966**, *88* (22), 5180−5185.

(25) La Mar, G. N.; Sacconi, L. Proton Magnetic Resonance Studies of High-Spin Nickel(II) Complexes with Pentadentate Schiff Bases. *J. Am. Chem. Soc.* **1967**, *89* (10), 2282−2291.

(26) Bertini, I.; Luchinat, C. *NMR of Paramagnetic Molecules in Biological Systems*; Benjamin/Cummings: Menlo Park, CA, 1986.

(27) Luchinat, C.; Steuernagel, S.; Turano, P. Application of 2D-NMR Techniques to Paramagnetic Systems. *Inorg. Chem.* **1990**, *29*, 4351−4353.

(28) Cerofolini, L.; Silva, J. M.; Ravera, E.; Romanelli, M.; Geraldes, C. F. G. C.; Macedo, A. L.; Fragai, M.; Parigi, G.; Luchinat, C. How Do Nuclei Couple to the Magnetic Moment of a Paramagnetic Center? A New Theory at the Gauntlet of the Experiments. *J. Phys. Chem. Lett.* **2019**, *10* (13), 3610−3614.

(29) Parigi, G.; Benda, L.; Ravera, E.; Romanelli, M.; Luchinat, C. Pseudocontact Shifts and Paramagnetic Susceptibility in Semiempirical and Quantum Chemistry Theories. *J. Chem. Phys.* **2019**, *150* (14), 144101.

(30) Benda, L.; Mareš, J.; Ravera, E.; Parigi, G.; Luchinat, C.; Kaupp, M.; Vaara, J. Pseudo-Contact NMR Shifts over the Paramagnetic Metalloprotein CoMMP-12 from First Principles. *Angew. Chem., Int. Ed.* **2016**, *55* (47), 14713−14717.

(31) Mareš, J.; Vaara, J. *Ab Initio* Paramagnetic NMR Shifts *via* Point-Dipole Approximation in a Large Magnetic-Anisotropy Co(II) Complex. *Phys. Chem. Chem. Phys.* **2018**, *20* (35), 22547−22555.

(32) Chyba, J.; Novák, M.; Munzarová, P.; Novotný, J.; Marek, R. Through-Space Paramagnetic NMR Effects in Host-Guest Complexes: Potential Ruthenium(III) Metallodrugs with Macrocyclic Carriers. *Inorg. Chem.* **2018**, *57* (15), 8735−8747.

(33) Srb, P.; Svoboda, M.; Benda, L.; Lepšík, M.; Tarábek, J.; Šícha, V.; Grüner, B.; Grantz-Šašková, K.; Brynda, J.; Řezáčová, P.; Konvalinka, J.; Veverka, V. Capturing a Dynamically Interacting Inhibitor by Paramagnetic NMR Spectroscopy. *Phys. Chem. Chem. Phys.* **2019**, *21* (10), 5661−5673.

(34) Lang, L.; Ravera, E.; Parigi, G.; Luchinat, C.; Neese, F. Solution of a Puzzle: High-Level Quantum-Chemical Treatment of Pseudocontact Chemical Shifts Confirms Classic Semiempirical Theory. *J. Phys. Chem. Lett.* **2020**, *11*, 8735−8744.

(35) McConnell, H. M.; Robertson, R. E. Isotropic Nuclear Resonance Shifts. *J. Chem. Phys.* **1958**, *29* (6), 1361−1365.

(36) Kurland, R. J.; McGarvey, B. R. Isotropic NMR Shifts in Transition Metal Complexes: Calculation of the Fermi Contact and Pseudocontact Terms. *J. Magn. Reson.* **1970**, *2*, 286−301.

(37) Orioli, P.; Di Vaira, M.; Sacconi, L. Crystal and Molecular Structure of the Nickel(II) Complex with the Pentadentate Ligand Bis(Salicylidene-. Gamma.-Iminopropyl)Methylamine. *Inorg. Chem.* **1971**, *10* (3), 553−558.

(38) Becke, A. D. A New Mixing of Hartree-Fock and Local Density-functional Theories. *J. Chem. Phys.* **1993**, *98* (2), 1372−1377.

(39) Lee, C.; Yang, W.; Parr, R. G. Development of the Colle-Salvetti Correlation-Energy Formula into a Functional of Electron Density. *Phys. Rev. B: Condens. Matter Mater. Phys.* **1988**, *37*, 785−789.

(40) Vosko, S. H.; Wilk, L.; Nusair, M. Accurate Spin-Dependent Electron Liquid Correlation Energies for Local Spin Density Calculations: A Critical Analysis. *Can. J. Phys.* **1980**, *58* (8), 1200−1211.

(41) Stephens, P. J.; Devlin, F. J.; Chabalowski, C. F.; Frisch, M. J. Ab Initio Calculation of Vibrational Absorption and Circular Dichroism Spectra Using Density Functional Force Fields. *J. Phys. Chem.* **1994**, *98* (45), 11623−11627.

(42) Schäfer, A.; Huber, C.; Ahlrichs, R. Fully Optimized Contracted Gaussian Basis Sets of Triple Zeta Valence Quality for Atoms Li to Kr. *J. Chem. Phys.* **1994**, *100* (8), 5829−5835.

(43) Weigend, F.; Ahlrichs, R. Balanced Basis Sets of Split Valence, Triple Zeta Valence and Quadruple Zeta Valence Quality for H to Rn: Design and Assessment of Accuracy. *Phys. Chem. Chem. Phys.* **2005**, *7* (18), 3297−3305.

(44) Grimme, S.; Antony, J.; Ehrlich, S.; Krieg, H. A Consistent and Accurate Ab Initio Parametrization of Density Functional Dispersion Correction (DFT-D) for the 94 Elements H-Pu. *J. Chem. Phys.* **2010**, *132* (15), 154104.

(45) Grimme, S.; Ehrlich, S.; Goerigk, L. Effect of the Damping Function in Dispersion Corrected Density Functional Theory. *J. Comput. Chem.* **2011**, *32* (7), 1456−1465.

(46) Kendall, R. A.; Früchtl, H. A. The Impact of the Resolution of the Identity Approximate Integral Method on Modern Ab Initio Algorithm Development. *Theor. Chem. Acc.* **1997**, *97* (1), 158−163.

(47) Vahtras, O.; Almlöf, J.; Feyereisen, M. W. Integral Approximations for LCAO-SCF Calculations. *Chem. Phys. Lett.* **1993**, *213* (5), 514−518.

(48) Barone, V.; Cossi, M. Quantum Calculation of Molecular Energies and Energy Gradients in Solution by a Conductor Solvent Model. *J. Phys. Chem. A* **1998**, *102* (11), 1995−2001.

(49) Neese, F. The ORCA Program System. *Wiley Interdiscip. Rev.: Comput. Mol. Sci.* **2012**, *2* (1), 73−78.

(50) Neese, F. Software Update: The ORCA Program System, Version 4.0. *Wiley Interdiscip. Rev.: Comput. Mol. Sci.* **2018**, *8* (1), No. e1327.

(51) Roos, B. O.; Taylor, P. R.; Sigbahn, P. E. M. A Complete Active Space SCF Method (CASSCF) Using a Density Matrix Formulated Super-CI Approach. *Chem. Phys.* **1980**, *48* (2), 157−173.

(52) Siegbahn, P. E. M.; Almlöf, J.; Heiberg, A.; Roos, B. O. The Complete Active Space SCF (CASSCF) Method in a Newton-Raphson Formulation with Application to the HNO Molecule. *J. Chem. Phys.* **1981**, *74* (4), 2384−2396.

(53) Angeli, C.; Cimiraglia, R. Multireference Perturbation Configuration Interaction V. Third-Order Energy Contributions in the Møller-Plesset and Epstein-Nesbet Partitions. *Theor. Chem. Acc.* **2002**, *107* (5), 313−317.

(54) Angeli, C.; Cimiraglia, R.; Evangelisti, S.; Leininger, T.; Malrieu, J.-P. Introduction of N-Electron Valence States for Multireference Perturbation Theory. *J. Chem. Phys.* **2001**, *114* (23), 10252−10264.

(55) Atanasov, M.; Aravena, D.; Suturina, E.; Bill, E.; Maganas, D.; Neese, F. First Principles Approach to the Electronic Structure, Magnetic Anisotropy and Spin Relaxation in Mononuclear 3d-Transition Metal Single Molecule Magnets. *Coord. Chem. Rev.* **2015**, *289−290*, 177−214.

(56) Schäfer, A.; Huber, C.; Ahlrichs, R. Fully Optimized Contracted Gaussian Basis Sets of Triple Zeta Valence Quality for Atoms Li to Kr. *J. Chem. Phys.* **1994**, *100* (8), 5829−5835.

(57) Weigend, F.; Ahlrichs, R. Balanced Basis Sets of Split Valence, Triple Zeta Valence and Quadruple Zeta Valence Quality for H to Rn:

Design and Assessment of Accuracy. *Phys. Chem. Chem. Phys.* **2005**, *7* (18), 3297.

(58) Hess, B. A. Relativistic Electronic-Structure Calculations Employing a Two-Component No-Pair Formalism with External-Field Projection Operators. *Phys. Rev. A: At., Mol., Opt. Phys.* **1986**, *33* (6), 3742−3748.

(59) Neese, F. Efficient and Accurate Approximations to the Molecular Spin-Orbit Coupling Operator and Their Use in Molecular g-Tensor Calculations. *J. Chem. Phys.* **2005**, *122* (3), 034107.

(60) Neese, F.; Wolf, A.; Fleig, T.; Reiher, M.; Hess, B. A. Calculation of Electric-Field Gradients Based on Higher-Order Generalized Douglas-Kroll Transformations. *J. Chem. Phys.* **2005**, *122* (20), 204107.

(61) Visscher, L.; Dyall, K. G. Dirac-Fock Atomic Electronic Structure Calculations Using Different Nuclear Charge Distributions. *At. Data Nucl. Data Tables* **1997**, *67* (2), 207−224.

(62) Bertini, I.; Luchinat, C.; Parigi, G.; Ravera, E. *Solution NMR of Paramagnetic Molecules: Applications to Metallobiomolecules and Models*; Elsevier: Amsterdam, 2017.

(63) Neese, F. Theoretical Study of Ligand Superhyperfine Structure. Application to Cu(II) Complexes. *J. Phys. Chem. A* **2001**, *105* (17), 4290−4299.

(64) Neese, F. Metal and Ligand Hyperfine Couplings in Transition Metal Complexes: The Effect of Spin-Orbit Coupling as Studied by Coupled Perturbed Kohn-Sham Theory. *J. Chem. Phys.* **2003**, *118* (9), 3939−3948.

(65) Singh, S. K.; Atanasov, M.; Neese, F. Challenges in Multi-reference Perturbation Theory for the Calculations of the G-Tensor of First-Row Transition-Metal Complexes. *J. Chem. Theory Comput.* **2018**, *14* (9), 4662−4677.

(66) Neese, F. Prediction of Electron Paramagnetic Resonance *g* Values Using Coupled Perturbed Hartree-Fock and Kohn-Sham Theory. *J. Chem. Phys.* **2001**, *115* (24), 11080−11096.

(67) Bertini, I.; Capozzi, F.; Luchinat, C.; Piccioli, M.; Vila, A. J. The Fe_4S_4 Centers in Ferredoxins Studied through Proton and Carbon Hyperfine Coupling. Sequence Specific Assignments of Cysteines in Ferredoxins from *Clostridium Acidi Urici* and *Clostridium Pasteurianum*. *J. Am. Chem. Soc.* **1994**, *116*, 651−660.

(68) Holm, R. H.; Kennepohl, P.; Solomon, E. I. Structural and Functional Aspects of Metal Sites in Biology. *Chem. Rev.* **1996**, *96* (7), 2239−2314.

(69) Bertini, I.; Dikiy, A.; Luchinat, C.; Macinai, R.; Viezzoli, M. S. ^{1}H NMR Study of the Reduced Cytochrome c' from *Rhodopseudomonas Palustris* containing a High Spin Iron(II) Heme Moiety. *Inorg. Chem.* **1998**, *37*, 4814−4821.

(70) Bertini, I.; Luchinat, C.; Parigi, G.; Walker, F. A. Heme Methyl ^{1}H Chemical Shifts as Structural Parameters in Some Low Spin Ferriheme Proteins. *JBIC, J. Biol. Inorg. Chem.* **1999**, *4*, 515−519.

(71) Shokhirev, N. V.; Walker, F. A. The Effect of Axial Ligand Plane Orientation on the Contact and Pseudocontact Shifts of Low-Spin Ferriheme Proteins. *JBIC, J. Biol. Inorg. Chem.* **1998**, *3* (6), 581−594.

(72) Rigamonti, L.; Bridonneau, N.; Poneti, G.; Tesi, L.; Sorace, L.; Pinkowicz, D.; Jover, J.; Ruiz, E.; Sessoli, R.; Cornia, A. A Pseudo-Octahedral Cobalt(II) Complex with Bispyrazolylpyridine Ligands Acting as a Zero-Field Single-Molecule Magnet with Easy Axis Anisotropy. *Chem. - Eur. J.* **2018**, *24* (35), 8857−8868.

(73) Briganti, M.; Garcia, G. F.; Jung, J.; Sessoli, R.; Le Guennic, B.; Totti, F. Covalency and Magnetic Anisotropy in Lanthanide Single Molecule Magnets: The DyDOTA Archetype. *Chem. Sci.* **2019**, *10* (30), 7233−7245.

(74) Krzystek, J.; Kohl, G.; Hansen, H.-B.; Enders, M.; Telser, J. Combining HFEPR and NMR Spectroscopies to Characterize Organochromium(III) Complexes with Large Zero-Field Splitting. *Organometallics* **2019**, *38* (9), 2179−2188.

(75) Suturina, E. A.; Maganas, D.; Bill, E.; Atanasov, M.; Neese, F. Magneto-Structural Correlations in a Series of Pseudotetrahedral $[Co^{II}(XR)_4]^{2-}$ Single Molecule Magnets: An Ab Initio Ligand Field Study. *Inorg. Chem.* **2015**, *54* (20), 9948−9961.

(76) Rantaharju, J.; Mareš, J.; Vaara, J. Spin Dynamics Simulation of Electron Spin Relaxation in $Ni^{2+}{}_{(Aq)}$. *J. Chem. Phys.* **2014**, *141* (1), 014109.

(77) Lunghi, A.; Totti, F.; Sessoli, R.; Sanvito, S. The Role of Anharmonic Phonons in Under-Barrier Spin Relaxation of Single Molecule Magnets. *Nat. Commun.* **2017**, *8* (1), 14620.

(78) Lunghi, A.; Sanvito, S. Multiple Spin-Phonon Relaxation Pathways in a Kramer Single-Ion Magnet. *arXiv:2005.12429 [cond-mat.mtrl-sci]* **2020**.

(79) Auer, A. A.; Tran, V. A.; Sharma, B.; Stoychev, G. L.; Marx, D.; Neese, F. A Case Study of Density Functional Theory and Domain-Based Local Pair Natural Orbital Coupled Cluster for Vibrational Effects on EPR Hyperfine Coupling Constants: Vibrational Perturbation Theory versus Ab Initio Molecular Dynamics. *Mol. Phys.* **2020**, *118* (19−20), No. e1797916.

(80) Vogler, S.; Dietschreit, J. C. B.; Peters, L. D. M.; Ochsenfeld, C. Important Components for Accurate Hyperfine Coupling Constants: Electron Correlation, Dynamic Contributions, and Solvation Effects. *Mol. Phys.* **2020**, *118* (19−20), No. e1772515.

(81) Sacconi, L.; Nannelli, P.; Nardi, N.; Campigli, U. Five-Coordination in Some Complexes of Nickel(II) with Schiff Bases, Formed from Salicylaldehydes and N,N-Substituted Ethylenediamines. II. *Inorg. Chem.* **1965**, *4* (7), 943−949.

(82) Sacconi, L.; Orioli, P. L.; Di Vaira, M. The Structure of Five-Coordinated High-Spin Complexes of Nickel(II) and Cobalt(II) with N-β-Diethylamineethyl-5-Chlorosalicylaldimine1. *J. Am. Chem. Soc.* **1965**, *87* (9), 2059−2059.

(83) Sacconi, L.; Ciampolini, M.; Speroni, G. P. Structure Mimicry in Solid Solutions of 3d Metal Complexes with N-Methylsalicylaldimine (Msal-Me). *J. Am. Chem. Soc.* **1965**, *87* (14), 3102−3106.

(84) Sacconi, L.; Bertini, I. Low- and High-Spin Five-Coordinate Cobalt(II) and Nickel(II) Complexes with Tris(2-Diphenylphosphinoethyl)Amine. *J. Am. Chem. Soc.* **1968**, *90* (20), 5443−5446.